Simultaneous low-frequency noise characterization of gate and drain currents in AlGaN/GaN high electron mobility transistors

Hemant Rao and Gijs Bosman[a)]
Department of Electrical and Computer Engineering, University of Florida, Gainesville, Florida 32611, USA

(Received 4 September 2009; accepted 13 October 2009; published online 20 November 2009)

Room temperature low frequency noise characteristics of gate and drain currents of an AlGaN/GaN high electron mobility transistor are reported. A Hooge parameter (α_H) ranging from 10^{-3} to 10^{-4} is extracted for drain current noise as a function of sheet carrier density. Gate current noise is simultaneously measured with drain noise both in the time and frequency domain. A weak correlation is seen between the drain and gate noise. Temporally unstable Lorentzian components on top of stable $1/f^{\gamma}$ noise are observed in the gate noise spectra which also show up as random telegraph signal noise in the time domain. It is proposed that the gate Schottky contact is of high quality but that electrically unstable point defects in the AlGaN layer are the cause of Lorentzians and random telegraph switching noise. © *2009 American Institute of Physics*.
[doi:10.1063/1.3259437]

I. INTRODUCTION

High electron mobility transistors (HEMTs) based on AlGaN/GaN have been widely touted as the next generation of wireless and high power devices. However, there are still unresolved problems pertaining to reliability which deter their large scale deployment. It is now well accepted that low frequency noise is closely linked to reliability and can give early indicators of device failure.[1] A large part of the current research effort in AlGaN/GaN HEMT reliability is concentrated on the poor gate contact and associated high leakage currents leading to problems such as drain current collapse, virtual gate effect, etc.[2] The gate leakage current has been shown to significantly enhance the drain noise in the AlGaN/GaN transistors and therefore, defect spectroscopy using drain noise alone becomes difficult. As a result an independent study of gate and drain noise simultaneously is required which to the authors' knowledge has not been performed until date. This paper demonstrates a comprehensive experimental setup developed to perform these simultaneous measurements on drain and gate noise as a function of respective bias (Fig. 1). The results of these measurements are used to identify individual noise sources in the vertical and lateral regions of gate stack and channel, respectively.

II. DEVICE DESCRIPTION AND EXPERIMENTAL SETUP

The device under study consisted of an 800 nm GaN buffer layer grown on a high resistivity Si substrate by metal organic chemical vapor deposition (MOCVD). A transition layer of AlN is employed for stress mitigation. The buffer is made semi-insulating by Fe doping which has been shown to pin the Fermi level in GaN at $E_c - 0.5$ eV.[3] On top of this buffer an 18 nm of unintentionally doped $Al_{0.26}Ga_{0.74}N$ barrier layer is grown by MOCVD and finally capped by 1.5 nm GaN. All the layers are undoped. A Schottky gate contact of 0.65 μm length is formed by depositing Ni/Au followed by a rapid thermal anneal (RTA). Ohmic contacts are created for drain and source regions by depositing Ti/Al followed by RTA. A SiN passivation is made by plasma-enhanced chemical-vapor deposition. The transistor has a gate width of 200 μm with 10 fingers corresponding to a gate periphery of 2 mm.

The setup for measuring the voltage drain noise uses a low noise voltage preamplifier (SRS560) connected at the drain terminal and a drain bias resistor at least 10 times higher than the small signal channel resistance. The gate noise setup required a different approach due to high leakage currents. Direct voltage amplification could not be done with a gate bias resistor. The gate current noise gets reflected to the drain noise via a voltage drop across the gate bias resistor and is subsequently enhanced by transconductance in the linear regime. Therefore, an ultralow noise op-amp AD797 was

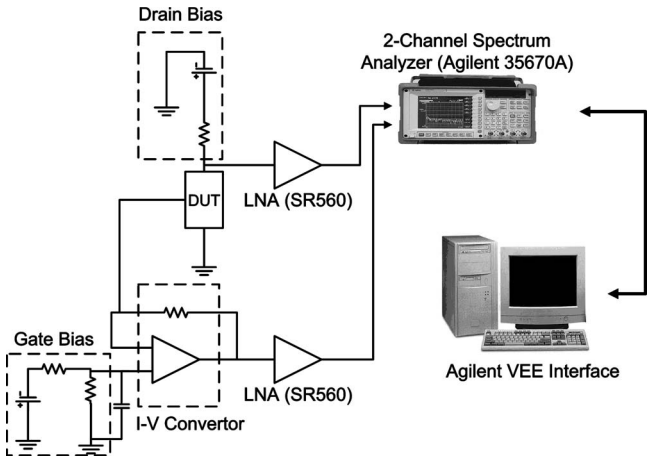

FIG. 1. Experimental setup for low frequency noise characterization. An ultralow noise op-amp (AD797) is employed as an *I-V* converter for gate current noise. Two SRS560 low noise voltage amplifiers are used to amplify gate and drain noise.

[a)]Electronic mail: bosman@ece.ufl.edu.

used to create an ac short circuit at the gate terminal and to convert gate current to voltage which in turn was amplified by a low noise voltage amplifier. Both these signals were simultaneously measured using the two-channel Agilent 35670A spectrum analyzer as shown in Fig. 1. It should be mentioned here that the main idea behind this approach is to create an ac short circuit at the gate terminal thus, preventing any circuit induced fluctuation to show in the drain noise. Interestingly most AlGaN/GaN HEMTs currently suffer from the problem of high gate leakage current and therefore, even a single channel drain noise measurement will show noise features of gate current if the gate is not properly ac shorted. A time domain noise measurement of both the channels or a spectral correlation measurement can determine if this problem exists.

Time domain random telegraph switching (RTS) noise was measured using an Agilent U2542A data acquisition unit sampled at 2 μs. DC characterization was performed by a HP4145B parameter analyzer and was limited to gate and drain *I-V*, and transconductance measurements. A *C-V* characterization using HP 4275A was also performed for the gate to source-drain diode to extract various device parameters of interest.

III. DC CHARACTERIZATION

Effective mobility of the channel was extracted from a combination of dc transconductance and *CV* profiling measurements. The mobility of the field-effect transistor (FET) in the linear regime was deduced using

$$\mu_N = \frac{L_G}{qn_S W_G R_{\mathrm{CH}}}, \tag{1}$$

where L_G, W_G are gate length and periphery, respectively, and R_{CH} is the channel resistance. Sheet carrier densities were extracted from the *C-V* characterization of the reverse bias gate to source-drain diode at 100 kHz using

$$n_S(V_G) = \frac{1}{q}\int_{V_P<V_T}^{V_G} C dV_G, \tag{2}$$

where V_P is taken below the threshold voltage. The calculated mobility values were between 180–415 $\mathrm{cm}^2/\mathrm{V\,s}$ for sheet concentrations ranging from 10^{11} to 10^{12} cm^{-2} and agreed well with results from other groups.[4] It was found that the mobility was a function of sheet carrier density which is also reported extensively.[5]

IV. DRAIN CURRENT NOISE

The device under test was biased in a common-source configuration at a constant low drain to source voltage of 80 mV. Drain current noise measurement is conducted by sweeping the gate voltage from −1.32 to −1.0 V at a constant V_{DS}=80 mV. The gate sweep was always over threshold voltage $V_T \approx -1.38$ V. The FET was kept in the linear regime and the resulting noise spectra were measured for the frequency range of 1 Hz–51.2 kHz at 300 K. The noise spectra were of the $1/f^{\gamma}$ type with the exponent $\gamma \sim 0.9$–0.85 varying inversely with the gate overdrive voltage shown in inset of Fig. 2. No distinct generation-recombination (GR) noise components could be seen. In the triode region, the channel consists of a gated part and ungated part of source, drain access regions. If the noises originating from these regions are assumed to be uncorrelated then the short circuited drain noise is

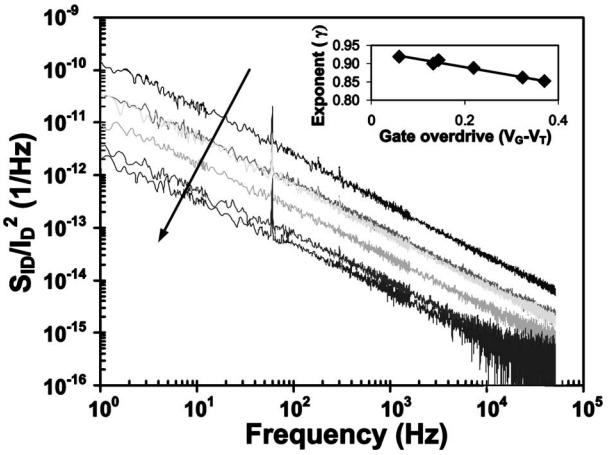

FIG. 2. Normalized drain current noise (S_{ID}/I_D^2) as a function of increasing (indicated by arrow) gate bias (V_G) of −1.32 to −1.01 V at V_{DS}=80 mV. Frequency exponent (γ) of the $1/f^{\gamma}$ noise varies from 0.9 to 0.85 as a function of increasing gate bias. Inset shows the measured frequency exponent γ as a function of gate overdrive voltage ($V_G - V_T$). The solid line is a theoretical best fit.

$$\frac{S_{\mathrm{ID}}}{I_D^2} = \frac{S_{\mathrm{RCH}}}{R_{\mathrm{CH}}^2}\left[\frac{R_{\mathrm{CH}}^2}{(R_S+R_D+R_{\mathrm{CH}})^2}\right] + \frac{S_{\mathrm{RD}}}{R_D^2}\left[\frac{R_D^2}{(R_S+R_D+R_{\mathrm{CH}})^2}\right] + \frac{S_{\mathrm{RS}}}{R_S^2}\left[\frac{R_S^2}{(R_S+R_D+R_{\mathrm{CH}})^2}\right], \tag{3}$$

where S_{RCH}, S_{RS}, and S_{RD} represent the uncorrelated resistance noise of the channel, source, and drain access regions, respectively. Only the channel noise is dependent on the gate bias and this feature is exploited to determine which term dominates in Eq. (3).

Figure 3 shows a plot of normalized drain current versus gate overdrive voltage ($V_G - V_T$). Two distinct regions of

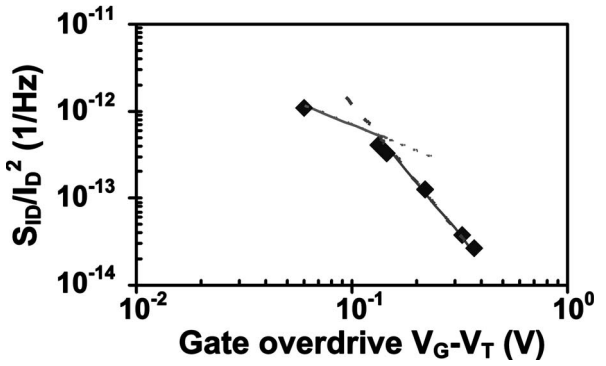

FIG. 3. Normalized drain current noise (S_{ID}/I_D^2) at 200 Hz as a function of gate overdrive voltage $V_G - V_T$. Solid lines are V_G^{-1} and V_G^{-3} fits on the measured data points for $0 < V_{G\text{-overdrive}} < 0.1$ and $V_{G\text{-overdrive}} > 0.1$, respectively.

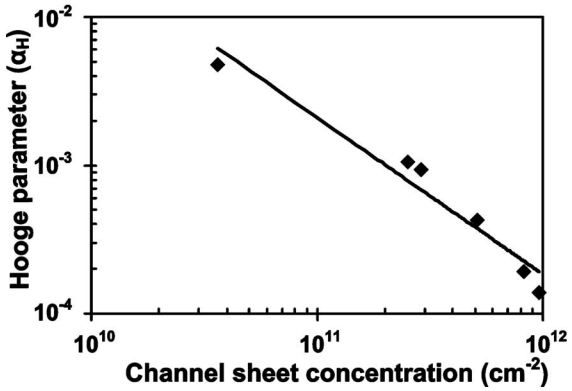

FIG. 4. Dependence of the Hooge parameter α_H on the sheet carrier concentration n_s (cm^{-2}). Solid line is a theoretical best fit for the measured data points; it shows $1/n_s$ dependence.

$S_{ID} \propto V_G^{-1}$ and V_G^{-3} dependence are observed in low and high gate voltage, respectively. This is a clear indicator that only the gated part of the channel noise is the dominant source.[6] Having determined the noise source, a Hooge parameter was calculated using the classical phenomenological equation

$$S_{ID}(f) = \frac{q\mu_n \alpha_H I_D V_D}{L_G^2 f}. \tag{4}$$

As seen in Fig. 4 the Hooge parameter associated with the gated part of the channel varies from $\approx 10^{-3}$ to 10^{-4} and shows an inverse dependence with the sheet carrier concentration. These values indicate that the noise from the access regions is still lower indicating the maturing of Ohmic contact technology in nitride-based materials. Also the temporal stability of the noise indicates a good quality of AlGaN/GaN interface. The inverse dependence of α_H with the sheet carrier concentration has been attributed to number fluctuations of carriers by thermally assisted tunneling in and out of the GaN donor states.[7] A temperature-based measurement was not performed which is essential to verify this claim. Interestingly, the frequency exponent $\gamma \propto 1/V_G$ dependence (see inset of Fig. 2) is in contradiction to silicon n-(metal-oxide-semiconductor field-effect transistors (MOSFETs) where band bending creates an increase in low frequency traps and $\gamma \propto V_G$.[8] On the other hand donor states in GaN can create this inverse dependence and therefore they may be responsible for the $1/f$ noise.

V. GATE CURRENT NOISE

Gate current noise is measured simultaneously with the drain noise as a function of gate overdrive voltage at constant V_{DS} of 80 mV. Therefore, the inverted channel exists for the complete gate bias range of V_G from -1.3 to -1.0 V. In the dc case the gate metal semiconductor junction is reverse biased and vertical tunneling of electrons, Fig. 5, is expected to be the dominant current leakage mechanism in this regime.[9] Considering this, the electron transport is predominantly from gate to the channel region, and therefore the low frequency noise of the leakage current is directly probing the metal semiconductor contact quality and space-charge region traps in the AlGaN barrier layer. If it is assumed that the noise sources in the device are uncorrelated, the compact

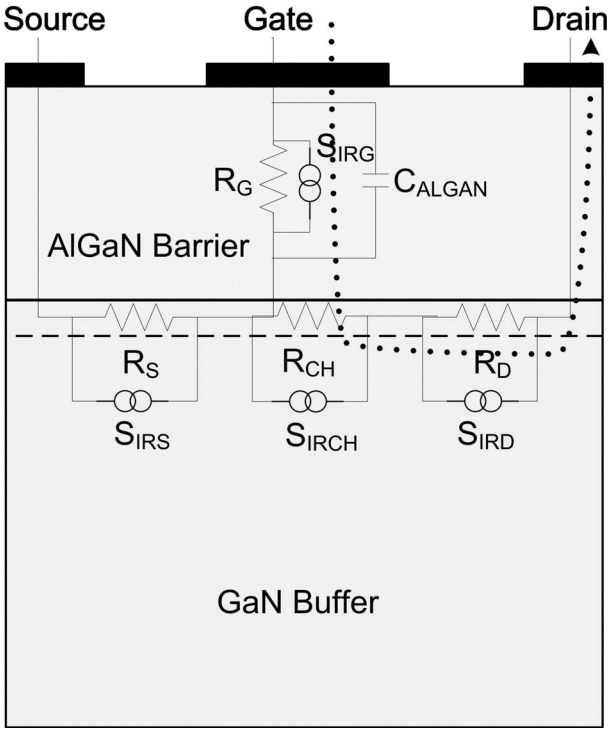

FIG. 5. Compact model of noise sources in the channel (S_{IRS}, S_{IRCH}, S_{IRD}) and gate region (S_{IRG}) of the device. The dashed line indicates the channel region at the AlGaN/GaN interface. The dotted line indicates the electron current leakage path for strong inversion and low drain bias.

noise model of the device can be constructed as shown in Fig. 5. The gate current flows from drain to gate through the channel therefore, the short circuit current fluctuation measured at the gate terminal is,

$$\frac{S_{IG}}{I_G^2} = \frac{S_{rg}}{R_G^2}\left[\frac{R_G^2}{(R_G+R_D+R_{CH})^2}\right] + \frac{S_{RCH}}{R_{CH}^2}\left[\frac{R_{CH}^2}{(R_G+R_D+R_{CH})^2}\right] + \frac{S_{RD}}{R_D^2}\left[\frac{R_D^2}{(R_G+R_D+R_{CH})^2}\right], \tag{5}$$

where, S_{rg}, S_{RCH}, and S_{RD} represent the noise of gate, channel, and drain regions, respectively. Channel and drain resistances $R_{CH} \approx 18.5\ \Omega$, $R_D \approx 2.5\ \Omega$ at gate bias $V_G \approx -1.3$ V were determined from the differential transconductance characteristics of the FET. Differential gate resistance $R_G \approx 6.6\ M\Omega$ at $V_G \approx -1.3$ V and $V_{DS} = 80$ mV was determined from the reverse gate to source I-V characteristics. Since $R_G \gg (R_{CH}+R_D)$ Eq. (5) reduces to

$$\frac{S_{IG}}{I_G^2} \approx \frac{S_{rg}}{R_G^2}. \tag{6}$$

This indicates that the gate noise originates mainly from the gate stack region and channel noise is negligible.

A. 1/f noise

Gate current noise power spectra of the same device under identical bias conditions but carried out at different time

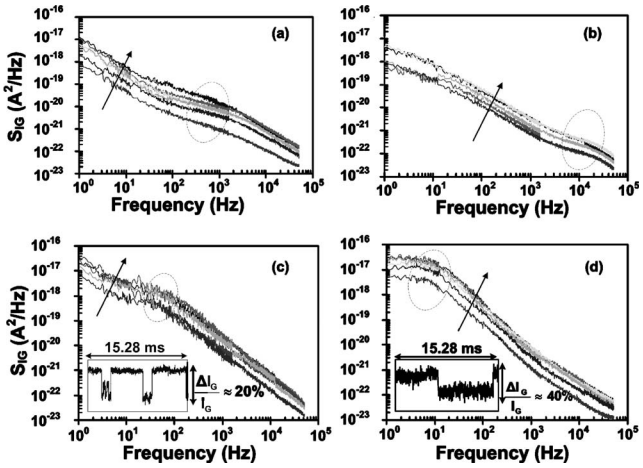

FIG. 6. Gate current noise spectra as a function of decreasing (indicated by arrow) gate bias (V_G) ranging from -1.32 to -1.01 V and $V_{DS}=80$ mV measured at four different time instances. A Lorentzian noise component without a time RTS noise is seen in (a) and (b). The insets in (c) and (d) show the corresponding RTS noise. The characteristic frequencies of all Lorentzians are different.

instances are shown in Fig. 6. In each case the spectrum has the form of $1/f^{\gamma}$ noise with a visible Lorentzian noise component on top of it. No high frequency roll off of noise was observed at any of the gate voltage in the measured frequency range of 1 Hz–51.2 kHz. As an indicator, the measured noise is at least three orders of magnitude higher than the shot noise ($2qI_G$) at 51.2 kHz, and therefore does not show up at high frequencies. Oftentimes a RTS noise was also observed in the time domain which manifested as a Lorentzian component in the frequency domain. The nature of the Lorentzian noise component is discussed in the next section. The $1/f^{\gamma}$ noise component of S_{IG} is extracted from the spectrum and plotted as function of gate direct current (I_G). A dependence of S_{IG} proportional to square of I_G is seen in Fig. 7. This $S_{IG} \propto I_G^2$ dependence is typical of a trap density fluctuation in the space charge region of the Schottky junction.[10] This $1/f^{\gamma}$ noise component was found to be temporally stable and reproducible. Therefore it may be argued that the gate Schottky contact is of high quality and does not degrade at least under normal bias conditions $V_{DS}<0.1$ V and $V_T<V_G<0$. Also, since the absolute magnitude of the $1/f^{\gamma}$ noise component remained the same the interface defect density does not change.

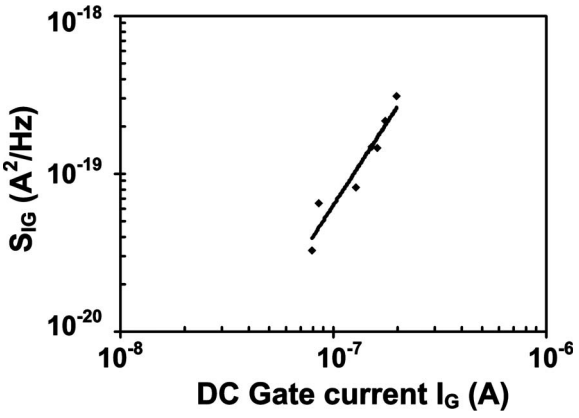

FIG. 7. Gate current noise as a function of dc gate current. Points are the measured values and solid line indicates the best fit dependence of $S_{IG} \propto I_G^2$.

B. RTS noise

As mentioned previously a nonrepeatable Lorentzian component was observed in the gate noise spectra when measured at different time instants under identical biasing conditions. Inset in Figs. 6(c) and 6(d) show the measured RTS noise in the time domain. The corner frequencies and respective time constants are different for both RTS. It was observed that repeating the same measurement at different time instances led to a change in the Lorentzian characteristic frequency (f_C) and magnitude. It "appeared" and "disappeared" randomly in the low and high frequency region of the spectra and no specific trend in the frequency drift could be observed. On the contrary, the background $1/f^{\gamma}$ noise in all those measurements remained stable and showed the same I_G dependence. This nonrepeatable Lorentzian and a repeatable $1/f^{\gamma}$ noise showed up in all the measurements. It is concluded that the gate fluctuation is actually a sum of two uncorrelated noise sources. The nonrepeatable Lorentzian component is an indicator of an unstable defect which migrates under device operation and shows up in the spectra at different locations and magnitude when it electrically interacts with the gate current. It is known that high electrical fields of the order of a few MV/cm are present in the AlGaN/GaN heterostructure due to spontaneous and piezoelectric polarization which are ordinarily not present in silicon MOSFETs in the off state. These are further enhanced by the applied gate bias during device operation. Also reported is the phenomenon that new defect centers can be generated via inverse piezoelectric effect for high fields under the gate stack.[11] The dominant defect centers in these devices consist of gallium and nitrogen vacancies which are known to be inherently unstable and exist in various metastable states with relatively small migration barrier in some cases.[12]

Therefore, it can be easily proposed that an unstable defect center in AlGaN barrier layer can migrate under the influence of these factors or by a complex interplay of them like electric field-induced mechanical strain. A migrated defect when interacting with the electron tunneling path will show up in the noise spectra as a Lorentzian. If this defect center happens to be at a strategic location, it will modulate the current pathway and show up as a RTS noise. Since it is believed that the dominant gate leakage mechanism in these devices is via dislocation spots, often a defect center located close to these dislocations will enable electron trapping and detrapping which will modulate the current and create large relative RTS noise. In all other cases it will lead to a Lorentzian component in the noise spectra. It was observed that most times the RTS noise showed a relative large fluctuation of $\Delta I_G/I_G$ between 20% and 40%. This behavior is consistent with a localized nature of gate current leakage. If it is assumed that the defect center responsible for modulating the dislocation current "blocks" the complete electron leakage pathway in that region, then a crude estimate of dislocation density can be extracted from the relative amplitude of the

RTS noise. In this case, a dislocation density of less than 10^6 cm^{-2} is deduced which is being reported in current state-of-the-art AlGaN/GaN HEMT devices.[13]

VI. SUMMARY

In conclusion, fundamental noise sources are identified in AlGaN/GaN HEMTs. It is found that there is an extremely weak correlation between gate and drain current noise. Drain current mainly stems from the gated channel region and shows a stable $1/f^{\gamma}$ noise without distinct GR noise components. A low value of Hooge parameter 10^{-4} is determined for it. On the other hand, gate current noise also exhibits a $1/f^{\gamma}$ noise with $S_{IG} \propto I_G^2$ dependence but shows in addition distinct Lorentzian components. Often these Lorentzians are so dominant that they show up as RTS noise in the time domain. These Lorentzians are found to be temporally unstable and their noise sources migrate under device operation whereas the background $1/f^{\gamma}$ noise is stable. It is proposed that the Schottky contact is of high quality and does not degrade under device operation but factors such as high electric fields, low defect migration barriers, high mechanical strain via inverse piezo-electric effect in the AlGaN/GaN system create a possibility whereby, defect centers in AlGaN barrier evolve spatially or change their energy locations. The exact nature of this migration needs to be explored further possibly by studying low frequency noise under systematically applied electrical stress to the gate stack. This makes the study of low frequency noise an extremely sensitive tool to study device reliability under realistic bias conditions.

ACKNOWLEDGMENTS

This work was supported by AFOSR MURI Grant (Grant No. FA9550-08-1-0264).

[1] E. Simoen and C. Claeys, Semicond. Sci. Technol. **14**, R61 (1999).
[2] H. Hasegawa, T. Inagaki, S. Ootomo, and T. Hashizume, Proceedings of the 30th Conference on the Physics and Chemistry of Semiconductor Interfaces, Salt Lake City, UT, 2003 (unpublished), pp. 1844–1855.
[3] A. Y. Polyakov, N. B. Smirnov, A. V. Govorkov, N. V. Pashkova, A. A. Shlensky, S. J. Pearton, M. E. Overberg, C. R. Abernathy, J. M. Zavada, and R. G. Wilson, J. Appl. Phys. **93**, 5388 (2003).
[4] S. L. Rumyantsev, N. Pala, M. S. Shur, R. Gaska, M. E. Levinshtein, P. A. Ivanov, M. A. Khan, G. Simin, X. Hu, and J. Yang, Semicond. Sci. Technol. **17**, 476 (2002).
[5] N. G. Weimann, L. F. Eastman, D. Doppalapudi, H. M. Ng, and T. D. Moustakas, J. Appl. Phys. **83**, 3656 (1998).
[6] J.-M. Peransin, P. Vignaud, D. Rigaud, and L. K. J. Vandamme, IEEE Trans. Electron Devices **37**, 2250 (1990).
[7] S. L. Rumyantsev, Y. Deng, E. Borovitskaya, A. Dmitriev, W. Knap, N. Pala, M. S. Shur, M. E. Levinshtein, M. Asif Khan, G. Simin, J. Yang, and X. Hu, J. Appl. Phys. **92**, 4726 (2002).
[8] Z. Celik-Butler and T. Y. Hsiang, Solid-State Electron. **30**, 419 (1987).
[9] E. J. Miller, X. Z. Dang, and E. T. Yu, J. Appl. Phys. **88**, 5951 (2000).
[10] T. S. Hsu, IEEE Trans. Electron Devices **17**, 496 (1970).
[11] J. Joh and J. A. del Alamo, Proceedings of the Electron Devices Meeting, 2006. IEDM '06. International, 2006 (unpublished), pp. 1–4.
[12] S. Limpijumnong and C. G. Van de Walle, Phys. Rev. B **69**, 035207 (2004).
[13] D. J. Ewing, M. A. Derenge, P. B. Shah, U. Lee, T. S. Zheleva, and K. A. Jones, J. Vac. Sci. Technol. B **26**, 1368 (2008).